Inorganic Chemistry

Article

pubs.acs.org/IC

Dinuclear Nickel Complexes in Five States of Oxidation Using a Redox-Active Ligand

You-Yun Zhou, Douglas R. Hartline, Talia J. Steiman, Phillip E. Fanwick, and Christopher Uyeda*

Department of Chemistry, Purdue University, West Lafayette, Indiana 47907, United States

Supporting Information

ABSTRACT: Redox-active nitrogen donor ligands have exhibited broad utility in stabilizing transition metal complexes in unusual formal oxidation states and enabling multielectron redox reactions. In this report, we extend these principles to dinuclear complexes using a naphthyridine−diimine (NDI) framework. Treatment of ($^{i\text{-Pr}}$NDI) with $Ni(COD)_2$ (2.0 equiv) yields a Ni(I)−Ni(I) complex in which the two metal centers form a single bond and the ($^{i\text{-Pr}}$NDI) ligand is doubly reduced. A homologous series of ($^{i\text{-Pr}}$NDI)Ni_2 complexes in five oxidation states were synthesized and structurally characterized. Across this series, the ligand ranges from a neutral state in the most oxidized member to a dianionic state in the most reduced. The interplay between metal- and ligand-centered redox activity is interrogated using a variety of experimental techniques in combination with density functional theory models.

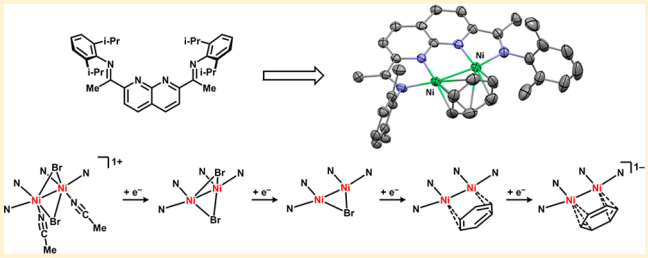

INTRODUCTION

Mononuclear complexes of Ni, Pd, and Pt feature prominently as redox catalysts in organic synthesis.[1] In the odd oxidation states, these transition metals exhibit a propensity to form diamagnetic dimers through metal−metal bonding. Several examples of group 10 M(I)−M(I) and M(III)−M(III) species have now been structurally characterized.[2] The significance of these bimetallic structures to carbon−carbon and carbon−heteroatom coupling reactions has been highlighted recently by the identification of Pd(III)−Pd(III) dimers as intermediates in oxidative C−H functionalizations[3] and the demonstration that Ni(I)−Ni(I) dimers can mediate C−C bond formation.[4] These processes raise the intriguing possibility that new pathways for coupling reactions might be discovered using complexes of higher nuclearity in which redox activity or substrate binding can span multiple metal centers.[5]

While complexes featuring bonding interactions between two Ni(I) centers have significant precedence,[4,6] the scope of redox chemistry that is known for these bimetallic units is relatively limited in comparison to their monometallic counterparts. Platforms that allow Ni−Ni bonds to be stabilized in multiple oxidation states are particularly rare. Among the few examples are the Ni_2(dppm)$_2$ cradle complexes studied by Kubiak for electrocatalytic CO_2 reduction[6e] and the Ni_2(*p*-terphenyldiphosphine) complexes reported by Agapie.[6c] Both cases make use of strong field phosphine ligands in combination with bridging carbonyls or isonitriles.

We are currently pursuing the synthesis of reactive and coordinatively unsaturated metal−metal bonds that are capable of engaging in multielectron redox processes. Nitrogen donor ligands with extended π-systems (e.g., pyridine−diimines, pyridine−bis(oxazolines), α-diimines, and iminopyridines) have been demonstrated to greatly expand the scope of accessible oxidation states in mononuclear transition metal complexes by acting as electron reservoirs at mildly reducing potentials.[7] This property has been effectively exploited in order to develop catalysts for which redox activity is primarily ligand-based rather than metal-based.[8] Nickel complexes of these ligands are useful for an array of C−C cross-coupling reactions,[1a,9] including those that are enantioselective.[10] Herein, we describe a naphthyridine diimine (NDI) ligand system (Figure 1) that confers a broader range of redox chemistry to dinuclear Ni complexes that has previously been observed using nonredox-active, strong field ligands. ($^{i\text{-Pr}}$NDI)Ni_2 complexes have been characterized in five states of oxidation, and the role of ligand-centered redox in affording stability to this series is discussed.

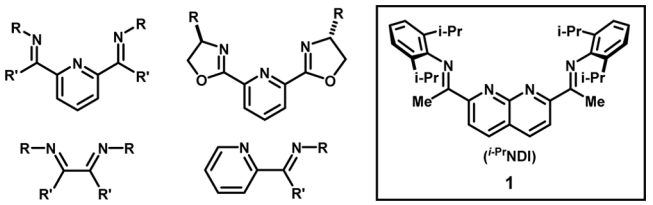

Figure 1. Mononucleating and binucleating redox-active ligands.

Received: August 28, 2014
Published: October 22, 2014

dx.doi.org/10.1021/ic5020785 | *Inorg. Chem.* 2014, 53, 11770−11777

RESULTS AND DISCUSSION

Synthesis of a ($^{i\text{-Pr}}$NDI)Ni_2 Complex. The binucleating ($^{i\text{-Pr}}$NDI) ligand **1** was synthesized on multigram scales in 25% overall yield from commercially available starting materials.[11,12] Our initial metalation efforts targeted a low-valent dinickel complex. Accordingly, ($^{i\text{-Pr}}$NDI) **1** was treated with 2.0 equiv of $Ni(COD)_2$ in benzene. Immediately after mixing, the reaction solution developed a green color. ^{1}H NMR spectra acquired after a 5 min reaction time revealed a mixture of monometalated ($^{i\text{-Pr}}$NDI)Ni compounds. After 24 h, these intermediates converted to a single dark brown, diamagnetic species (**2**) with a spectrum that was consistent with a C_{2v}-symmetric dinuclear ($^{i\text{-Pr}}$NDI)Ni_2 structure. A sharp singlet at 4.54 ppm (^{13}C NMR: 79 ppm) was assigned to a bound equivalent of benzene that rotates rapidly on the NMR chemical shift time scale. Over the course of days at room temperature, exchange of the bound C_6H_6 with the C_6D_6 solvent was observed indicating that benzene is susceptible to substitution.

X-ray diffraction analysis of crystalline ($^{i\text{-Pr}}$NDI)$Ni_2(C_6H_6)$ **2** obtained from a concentrated pentane solution confirmed the presence of two nickel centers, which are separated by 2.496(1) Å (Figure 2). This relatively short distance is suggestive of a net

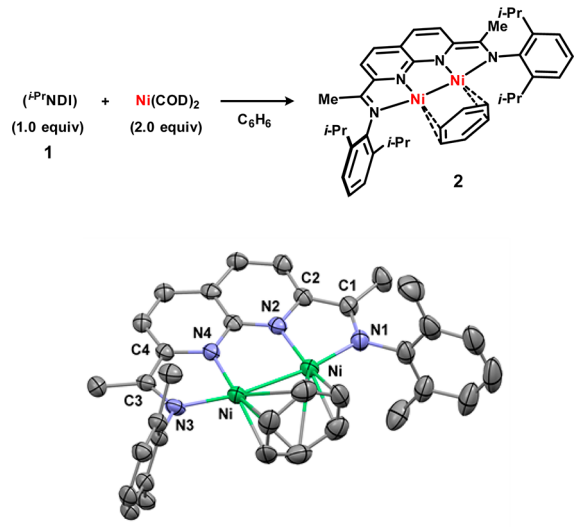

Figure 2. Synthesis and solid-state structure (ellipsoids at 50% probability) of ($^{i\text{-Pr}}$NDI)$Ni_2(C_6H_6)$ (**2**). Hydrogen atoms and *i*-Pr groups on the ($^{i\text{-Pr}}$NDI) ligand are truncated for clarity.

single bond and is within the range of crystallographically characterized Ni(I)−Ni(I) species.[2d,4a,c,6h,13] Correspondingly, the metrical parameters associated with the naphthyridine−diimine supporting ligand exhibit features of ligand-centered reduction: as compared to the neutral form of the ligand, the imine C−N and naphthyridine C_{ipso}−N distances are elongated, and the intervening C−C bonds are contracted (Table 1). Bond metrics for the two halves of the ligand are identical within error. Consistent with a reduced state for the bound ($^{i\text{-Pr}}$NDI) ligand, ^{1}H NMR resonances assigned to the naphthyridine ring and the imine methyl substituents are shifted upfield by approximately 2.5 and 0.7 ppm respectively relative to the free ligand.

Further details pertaining to the electronic structure of complex **2** were obtained from density functional theory (DFT) calculations (BP86/6-311G(d,p)). Two primarily ligand-based orbitals were identified: one that is symmetric with respect to rotation about the C_2 axis (Figure 3a, highest occupied molecular orbital (HOMO)) and one that is antisymmetric and higher in energy (Figure 3b, lowest unoccupied molecular orbital (LUMO)+1). Complex **2** exhibits an intense near-infrared (NIR) absorption band at 1040 nm (ε = 40 000 cm^{-1} M^{-1}). Preliminary time-dependent (TD) DFT calculations reproduce this feature (calculated: 985 nm) and suggest that it is primarily attributed to a ligand-based transition from the HOMO to the LUMO+1.

In support of a net Ni−Ni single bond for the ($^{i\text{-Pr}}$NDI)-$Ni_2(C_6H_6)$ complex **2**, an orbital with Ni−Ni σ-bonding character can be located at HOMO−6 (Figure 3c). The corresponding σ-antibonding combination (Figure 3d) is unoccupied (LUMO). Overall, the structural data, spectroscopic features, and computational model for **2** are highly consistent with a Ni(I)−Ni(I) and ($^{i\text{-Pr}}$NDI)$^{2-}$ oxidation state assignment.

An Electron Transfer Series of ($^{i\text{-Pr}}$NDI)Ni_2 Complexes. In tetrahydrofuran (THF) solution, the ($^{i\text{-Pr}}$NDI)$Ni_2(C_6H_6)$ complex **2** exhibits rich electrochemistry with two reductions (−2.24 and −2.86 V vs Cp_2Fe/Cp_2Fe^+) and two oxidations (−1.04 and −0.43 V) spanning a potential range of approximately 2.5 V (Figure 4a). The remarkably reversible redox behavior[14] observed by cyclic voltammetry prompted us to pursue the isolation and characterization of its reduced and oxidized congeners.

Reduction of ($^{i\text{-Pr}}$NDI)$Ni_2(C_6H_6)$ **2** using KC_8 (1.0 equiv) in THF yielded the S = 1/2 anionic complex **3** (Scheme 1). In the solid state (Figure 5a), the K^+ ion coordinates 3 equiv of THF and is located in proximity to the Ni centers (K−Ni: 3.369(1), 3.459(1) Å) and the nitrogen atoms of the naphthyridine ring (K−N: 2.951(3), 3.041(3) Å). The equivalent of C_6H_6 that spans the two Ni centers in the neutral complex **2** is retained upon reduction.

One- and two-electron oxidized products of ($^{i\text{-Pr}}$NDI)-$Ni_2(C_6H_6)$ **2** were accessible as the neutral halide complexes by treatment with 0.5 or 1.0 equiv of [*n*-Bu_4N]Br_3 respectively (Scheme 2). While these oxidation reactions allowed for product identification, analytically pure samples of the ($^{i\text{-Pr}}$NDI)Ni_2Br_2 complex **4** (Figure 5b) are more conveniently prepared by comproportionation of $Ni(COD)_2$ and $NiBr_2$ in the presence of an equimolar amount of the ($^{i\text{-Pr}}$NDI) ligand **1**. Notably, the resulting dark green product exhibits paramagnetically shifted ^{1}H NMR resonances and a room temperature, solution magnetic moment of 2.7 μB, suggestive of an S = 1 state. This result highlights the accessibility of bimetallic complexes with higher spin states using the relatively weak field ($^{i\text{-Pr}}$NDI) ligand system. By contrast, reported examples of phosphine-[4a,6h] or NHC-supported[13] dinickel complexes with bridging halides are diamagnetic. In the solid-state structure, the two bromide ligands are symmetrically bridged between the two Ni centers. The local geometry at Ni is pseudotetrahedral with a Ni−Ni distance (2.5316(7) and 2.5399(7) Å for the two molecules in the asymmetric unit) that is considerably elongated from that observed for complex **2**.

The ($^{i\text{-Pr}}$NDI)Ni_2Br_2 complex **4** was reduced to the violet, S = 1/2 monobromide complex **5** using Na/Hg (1.1 equiv). The bridging Br ligand moves into the plane defined by the naphthyridine−diimine π-system and two Ni centers (Figure 5c). The Ni−Ni distances (2.377(1) and 2.3718(9) Å for the two molecules in the asymmetric unit) are the shortest among the compounds that we have characterized with this ligand

dx.doi.org/10.1021/ic5020785 | Inorg. Chem. 2014, 53, 11770−11777

Table 1. Selected Bond Distances (Å) from Solid-State Structures of 1−6[a]

compound	Ni−Ni	Ni−N1 Ni−N3	Ni−N2 Ni−N4	C1−N1 C3−N3	C2−N2 C4−N4	C1−C2 C3−C4
1	–	–	–	1.279(2)	1.322(2)	1.500(2)
				1.279(2)	1.327(2)	1.494(3)
2	2.496(1)	1.955(5)	1.863(3)	1.332(6)	1.405(7)	1.413(6)
		1.965(4)	1.866(3)	1.335(5)	1.400(6)	1.418(7)
3	2.5947(7)	2.020(3)	1.911(3)	1.314(4)	1.409(4)	1.421(5)
		2.015(3)	1.905(3)	1.321(5)	1.423(5)	1.418(5)
4[b]	2.5316(7)	1.912(3)	1.925(4)	1.300(6)	1.357(5)	1.462(5)
	2.5399(7)	1.922(3)	1.925(4)	1.310(6)	1.344(5)	1.453(6)
5[c]	2.378(1)	1.956(4)	1.869(3)	1.304(5)	1.355(7)	1.449(7)
	2.371(1)	1.963(5)	1.875(3)	1.298(6)	1.367(6)	1.448(8)
		1.959(3)	1.882(3)	1.300(5)	1.355(6)	1.447(6)
		1.963(3)	1.874(3)	1.303(4)	1.371(5)	1.449(6)
6	2.525(1)	2.039(4)	2.026(4)	1.293(6)	1.331(6)	1.487(6)
		2.052(3)	2.021(3)	1.288(6)	1.329(5)	1.493(7)

[a]See Figure 2 for numbering scheme. [b]Two molecules in the asymmetric unit, each sits on a 2-fold axis. Metrical parameters for both are shown. [c]Two molecules in the asymmetric unit. Metrical parameters for both are shown.

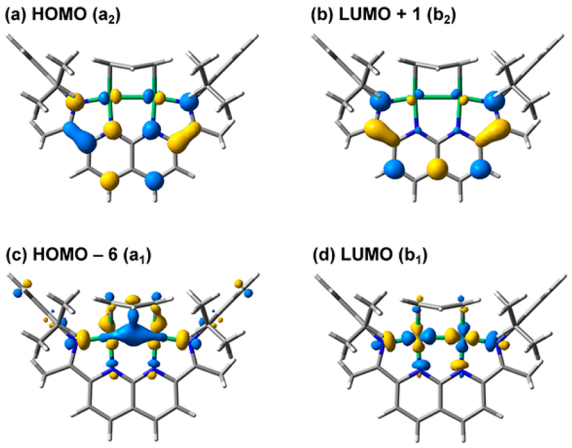

Figure 3. Selected Kohn−Sham orbitals (BP86/6-311G(d,p)) for the computationally optimized structure of ($^{i\text{-Pr}}$NDI)$Ni_2(C_6H_6)$ (**2**) with symmetry labels corresponding to the C_{2v} point group.

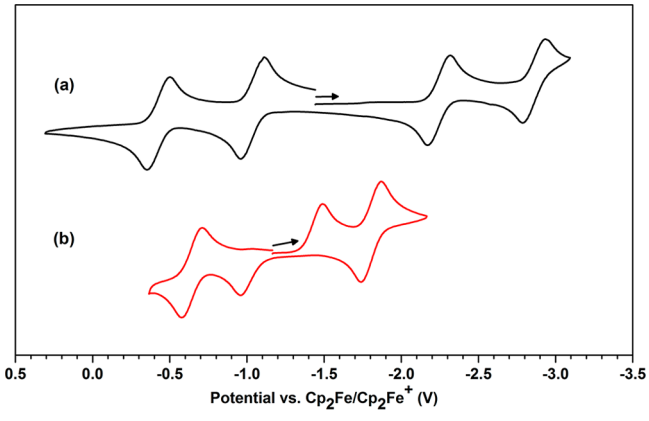

Figure 4. Cyclic voltammograms for (a) **2** and (b) **4** (0.2 M [*n*-Bu_4N][PF_6] supporting electrolyte in THF, glassy carbon working electrode, 100 mV/s scan rate). Scans begin at the open circuit potential and proceed in the indicated direction.

system. When **4** is reduced with 2.0 equiv of Na/Hg in the presence of C_6H_6, the ($^{i\text{-Pr}}$NDI)$Ni_2(C_6H_6)$ complex **2** is regenerated.

Scheme 1. Synthesis of $(THF)_3K(^{i\text{-Pr}}NDI)Ni_2(C_6H_6)$ (3)

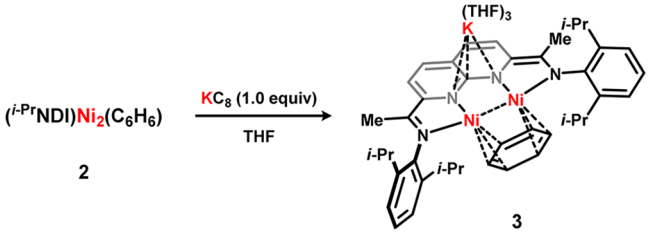

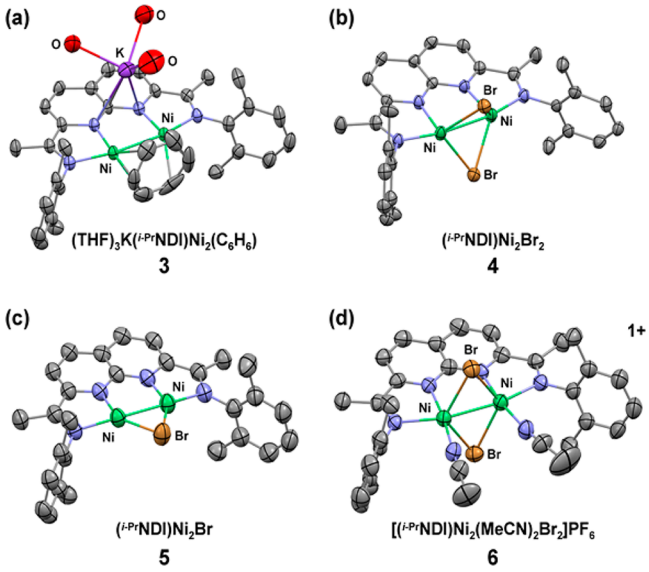

Figure 5. Solid-state structures (ellipsoids at 50% probability) for complexes (a) **3**, (b) **4**, (c) **5**, and (d) **6**. Hydrogen atoms, noncoordinated solvent molecules and anion, and portions of the ligand are truncated for clarity.

The effect of associating anionic halide ligands on the redox potentials of the ($^{i\text{-Pr}}$NDI)Ni_2 complexes was assessed by cyclic voltammetry (Figure 4b). The ($^{i\text{-Pr}}$NDI)Ni_2Br_2 complex **4** exhibits two reductions (−1.23 and −1.80 V vs Cp_2Fe/Cp_2Fe^+) that are shifted cathodically by approximately 800 mV relative to the corresponding couples for the ($^{i\text{-Pr}}$NDI)$Ni_2(C_6H_6)$ complex **2**. The first reduction wave is chemically reversible, but

dx.doi.org/10.1021/ic5020785 | Inorg. Chem. 2014, 53, 11770−11777

Scheme 2. Synthesis of ($^{i\text{-Pr}}$NDI)Ni_2 Bromide Complexes (4–6)

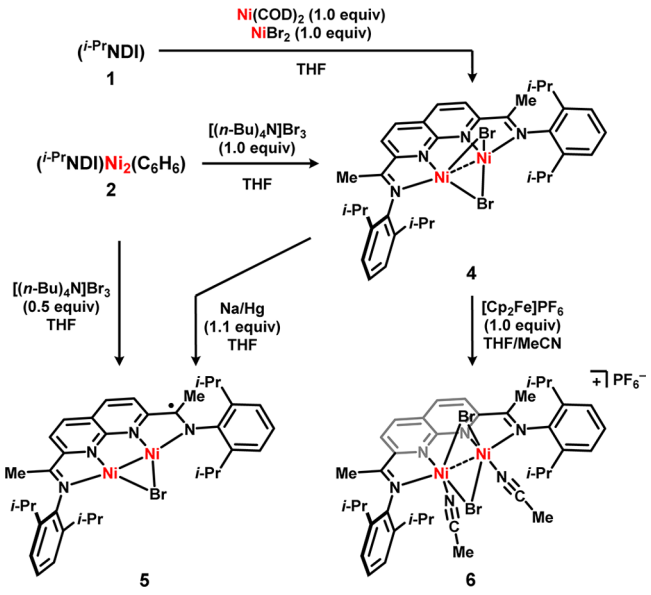

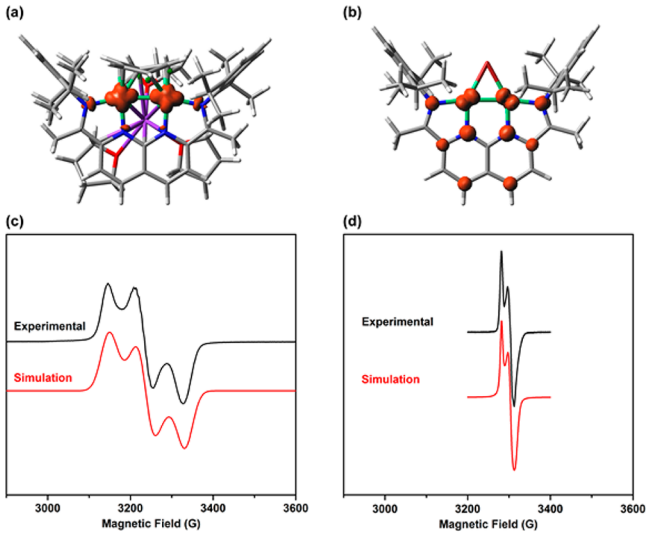

Figure 6. Calculated spin-density plots for (a) **3** and (b) **5**. Mulliken spin population for **3** Ni_2 = 0.90; Σ over ligand atoms = 0.07. Mulliken spin population for **5**: Ni_2 = 0.43; Σ over ligand atoms = 0.57. Frozen solution EPR spectra (125 K) for (c) **3** and (d) **5**. Simulated parameters for **3**: g_1 = 2.037, g_2 = 2.097, g_3 = 2.157. Simulated parameters for **5**: g_1 = 2.050, g_2 = 2.037, g_3 = 2.029.

exhibits a large peak-to-peak separation of 530 mV—likely an indication that reduction is accompanied by halide dissociation. Consistent with this interpretation, the reoxidation wave at −0.96 V is not observed when the scan is conducted in the anodic direction from the open circuit potential. Bromide binding also results in an additional reversible oxidation at −0.6 V that is not observed in the electrochemistry for **2**.

Chemical oxidation of the neutral dibromide complex **4** was carried out using $[Cp_2Fe]PF_6$ (1.0 equiv). In THF solution, this reaction yielded an aggregated $[(^{i\text{-Pr}}NDI)_2Ni_4Br_5]^+$ cluster in which the desired oxidation state was obtained, but the ($^{i\text{-Pr}}$NDI)Ni_2 units are dimerized through bridging bromides (see Supporting Information for XRD data). Control over nuclearity in this species was achieved by conducting the oxidation in the presence of MeCN. The resulting blue S = 3/2 species **6** (μ_{eff} = 4.1 μB, room temperature, MeCN solution) incorporates two equivalents of MeCN in the inner sphere—one bound to each Ni center.

Electronic Structure and the Role of Ligand-Centered Redox Activity. The isolation of a homologous series of complexes sharing a common ($^{i\text{-Pr}}$NDI)Ni_2 core provided us with a unique opportunity to probe the electronic structure of these dinuclear complexes in detail and assess the relative participation metal- and ligand-centered orbitals in their redox chemistry.

On the basis of its calculated electronic structure, reductions of complex **2** are expected to populate an orbital of Ni–Ni σ^* character, whereas oxidations would be predominantly ligand-centered. In support of this model, the Ni–Ni distance is elongated by 0.126 Å in the anionic complex **3** relative to the neutral complex **2**. The Ni–N distances also increase by approximately 0.05 Å on average upon reduction. The metalloradical character of **3** is corroborated by its frozen solution electron paramagnetic resonance (EPR) spectrum (125 K, THF, Figure 6c), which indicates a rhombic environment with significant anisotropy ($g_{max} - g_{min}$ = 0.12) and partially resolved hyperfine coupling due to the nitrogen donors.

By contrast, EPR spectra for the S = 1/2 monobromide complex **5** are consistent with a high degree of ligand radical character (Figure 6d): the g_{iso} of 2.041 from the room temperature solution spectrum is near the free electron value of 2.002, and the degree of anisotropy ($g_{max} - g_{min}$ = 0.021) in the frozen solution spectrum (125 K, 2-MeTHF) is relatively small. Accordingly, a majority of the calculated spin density by Mulliken population analysis is localized on the ligand atoms (Figure 6b), Σ over the ligand atoms: 0.57). While the high degree of covalency in the singly occupied molecular orbital precludes an unambiguous determination of integer oxidation states, the EPR data and DFT calculations suggest that a Ni(I)–Ni(I) and $(NDI)^{1-}$ formulation is favored.

The two most oxidized complexes, **4** and **6**, adopt higher spin states and exhibit Ni–Ni distances (2.5316(7) and 2.5399(7), Å respectively) that are elongated relative to the ($^{i\text{-Pr}}$NDI)-$Ni_2(C_6H_6)$ complex **2**. These trends in the Ni–Ni distances are well-reproduced by DFT calculations (calculated: 2.5142 and 2.5450 Å, respectively). For both complexes, computational models suggest that the higher spin states populate an orbital of Ni–Ni σ^* character, analogous to that shown in Figure 3d for **2**.

Successive oxidations from the ($^{i\text{-Pr}}$NDI)$Ni_2(C_6H_6)$ complex **2** cause a continuous progression in the naphthyridine C_{ipso}–N, imine C–N, and C_{ipso}–C_{imine} distances toward those characteristic of a neutral state. The most oxidized member of the series (**6**) exhibits key ligand bond metrics that approach those observed for free ($^{i\text{-Pr}}$NDI). Ligand bond distances for complexes **3** and **2** are nearly identical within error, consistent with the reduction of **2** being primarily metal-centered. These trends are illustrated in Figure 7. Across this series, the napthyridine C_{ipso}–N distances vary over a larger range (approximately 0.09 Å) than the imine C–N distances (approximately 0.05 Å). In accordance with this observation, the orbital coefficients associated with the napthyridine nitrogen and ipso carbon are greater than those associated with the imine nitrogen and carbon in the redox-active ligand

dx.doi.org/10.1021/ic5020785 | Inorg. Chem. 2014, 53, 11770–11777

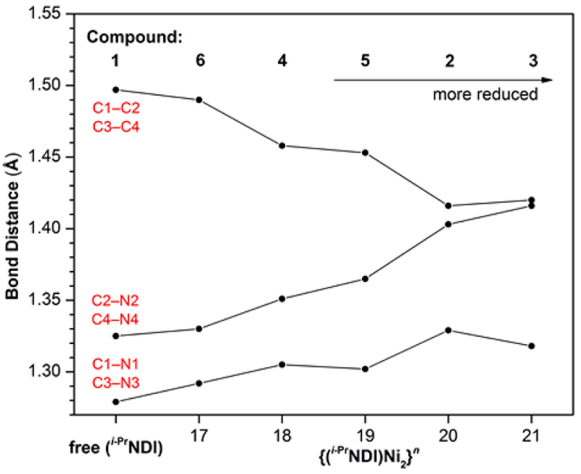

Figure 7. Summary of ligand bond metrics across the redox series. Average bond distances are plotted against *n*, which denotes the formal number of Ni 3d electrons without consideration for ligand-centered redox in analogy to the Enemark–Feltham notation for metal nitrosyl complexes. Metrics for the free ($^{i\text{-Pr}}$NDI) ligand (**1**) are shown for comparison as the leftmost set of data. Estimated standard deviations are ≤0.007 for all structures.

orbital (Figure 3a). Thus, far, we have not observed any cases where the ($^{i\text{-Pr}}$NDI) ligand is reduced by more than two electrons.

The redox chemistry of the ($^{i\text{-Pr}}$NDI)Ni_2 platform is summarized in the truncated molecular orbital diagram shown in Figure 8. Across the homologous series of Ni_2 complexes **2**–**6**, the ($^{i\text{-Pr}}$NDI) ligand adopts a neutral, anionic, or dianionic state through population of the ligand-centered orbital illustrated in Figure 3a. The remainder of the redox activity is centered on the dinickel fragment, which is best approximated as being in a Ni(I)–Ni(I) state for the intermediate members of the series, but gains or loses an additional electron in the most reduced or oxidized complexes, respectively.

CONCLUSIONS

In summary, we have established that (NDI)Ni_2 complexes can access a range of oxidation states by accommodating varying amounts of electron density in the π-system of the ligand. Thus, dinuclear nickel complexes can be isolated and characterized in five states of oxidation, representing a significant expansion in the scope of redox chemistry for Ni–Ni bonds.

As a step toward utilizing metal–metal bonds as robust active sites in catalysis, the NDI ligand has been demonstrated to span the dianionic and neutral states in the ($^{i\text{-Pr}}$NDI)$Ni_2(C_6H_6)$ and ($^{i\text{-Pr}}$NDI)Ni_2Br_2 complexes. These species can be readily interconverted by oxidation or reduction reactions, providing evidence that this platform might accommodate an array of well-defined oxidative addition and reductive elimination processes that preserve the Ni–Ni bond. This approach to multimetallic redox chemistry bears analogy to certain metalloenzymes for which ligands that bridge two metals are proposed to be redox active during catalytic turnover. For example, EPR studies conducted on the paramagnetic oxidized

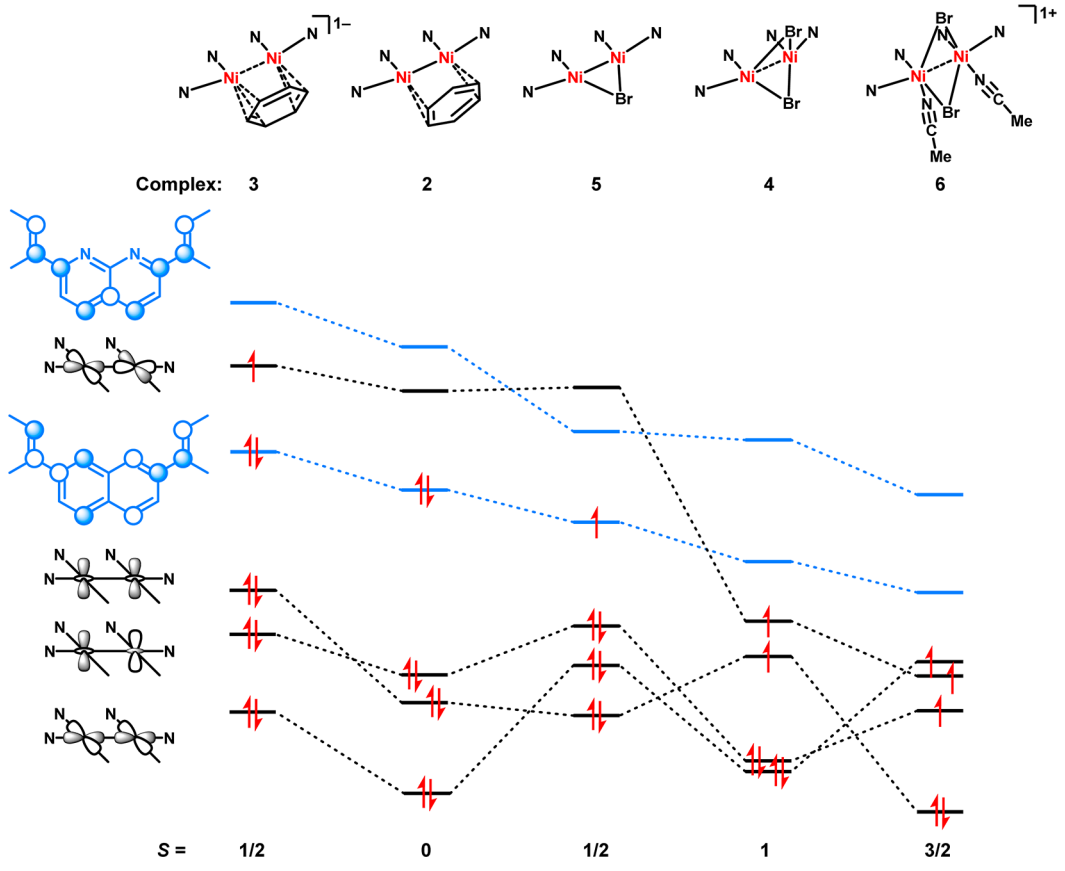

Figure 8. A truncated, qualitative MO diagram highlighting ligand-centered orbitals and metal-centered orbitals relevant to oxidation state assignments and Ni–Ni bonding. Relative energies and orbital assignments are based on DFT calculations (BP86/6-311G(d,p).

dx.doi.org/10.1021/ic5020785 | *Inorg. Chem.* 2014, 53, 11770–11777

state of NiFe hydrogenase place a significant fraction of the spin density on a bridging cysteine thiolate.[15] Ongoing efforts in our laboratory are directed toward exploiting the redox properties of (NDI)Ni_2 complexes in stoichiometric bond activations and catalysis.

EXPERIMENTAL SECTION

General Considerations. All manipulations were carried out using standard Schlenk or glovebox techniques under an atmosphere of N_2. Solvents were dried and degassed by passage through a column of activated alumina and sparging with N_2 gas. Deuterated solvents were purchased from Cambridge Isotope Laboratories, Inc., degassed, and stored over activated 3 Å molecular sieves prior to use. 2,7-diacetyl-1,8-naphthyridine was prepared according to previously reported procedures.[16] All other reagents and starting materials were purchased from commercial vendors and used without further purification unless otherwise noted. Elemental analyses were performed by Midwest Microlab (Indianapolis, IN).

Physical Methods. ^{1}H and ^{13}C NMR spectra were collected at room temperature on Varian 300 MHz NMR spectrometers. ^{1}H and ^{13}C NMR spectra are reported in parts per million relative to tetramethylsilane, using the residual solvent resonances as an internal standard. X-Band EPR spectra were recorded on a Bruker EMX EPR spectrometer and simulated using the Easyspin program.[17] UV−vis measurements were acquired on a Cary 100 UV/vis Spectrophotometer using a 1 cm two-window quartz cuvette. Electrochemical measurements were performed using a Pine WaveNow Potentiostat. Cyclic voltammograms were acquired using a glassy carbon working electrode (3 mm diameter disk) under an atmosphere of N_2. The potentials were internally referenced to the reversible $Cp_2Fe/[Cp_2Fe]^+$ couple.

X-ray Crystallography. Single-crystal X-ray diffraction studies were carried out at the Purdue X-ray crystallography facility on either a Nonius KappaCCD or Rigaku Rapid II diffractometer. Data were collected at 150 or 200 K using Mo Kα (λ = 0.710 73 Å) or Cu Kα (λ = 1.541 78 Å) radiation. Structures were solved by the direct method using SHELXT and refined against F^2 on all data by full-matrix least-squares. For complexes **2** and **5**, the SQUEEZE routine in the PLATON[18] program package was used to account for electron density in the solvent-accessible voids.

Computational Methods. DFT calculations were performed with the Gaussian 09 software package.[19] All geometries were fully optimized at the BP86/6-311G(d,p) level of DFT[20] using the XRD coordinates as input geometries. All stationary points were verified by frequency analysis. For complex **6**, the noncoordinated PF_6 anion was excluded from calculations. No other truncations were made to the calculated structures. All of the major structural trends (Ni−Ni distances, Ni−ligand distances, and ligand bond metrics relevant to the redox-active orbital) are well-reproduced at this level of theory. A systematic overestimation of the imine C−N distances by approximately 0.02 Å is observed across all structures. A full comparison of calculated and experimental bond distances from the XRD structures for **1**−**6** is included in the Supporting Information.

1,1′-(1,8-Naphthyridine-2,7-diyl)bis(*N*-(2,6-diisopropylphenyl)ethan-1-imine) ($^{i\text{-Pr}}$NDI) (1). 2,7-diacetyl-1,8-naphthyridine[16] (430 mg, 2.00 mmol, 1.00 equiv) was suspended in 10 mL of EtOH. 2,6-Diisopropylaniline (880 μL, 4.20 mmol, 2.10 equiv) was added by syringe. AcOH (10 μL) was added, and the reaction mixture was stirred at reflux under an atmosphere of N_2 for 48 h. The reaction mixture was cooled to room temperature and concentrated to dryness under reduced pressure. The residue was washed with four 2 mL portions of EtOH cooled to 0 °C. After drying under reduced pressure, ($^{i\text{-Pr}}$NDI) **1** (950 mg, 1.80 mmol, 89% yield) was isolated as a yellow powder. Single crystals suitable for XRD were obtained by slow cooling of a saturated solution of **1** in boiling EtOH. ^{1}H NMR (300 MHz, $CDCl_3$) δ 8.70 (d, J = 8.4 Hz, 2H), 8.37 (d, J = 8.5 Hz, 2H), 7.24−7.06 (m, 6H), 2.78 (sept, J = 6.9 Hz, 4H), 2.47 (s, 6H), 1.18 (d, J = 2.5 Hz, 12H), 1.15 (d, J = 2.6 Hz, 12H). ^{13}C NMR (75 MHz, $CDCl_3$) δ 167.3, 159.5, 154.7, 146.2, 137.1, 135.4, 124.2, 123.9, 123.0, 120.6, 28.7, 23.6, 23.2, 17.9. Anal. Calcd for **1** ($C_{36}H_{44}N_4$): C 81.16, H 8.32, N 10.52; found: C 81.09, H 8.25, N 10.54%.

($^{i\text{-Pr}}$NDI)$Ni_2(C_6H_6)$ (2). Under an atmosphere of N_2, a vial was charged with ($^{i\text{-Pr}}$NDI) **1** (107 mg, 0.200 mmol, 1.00 equiv), Ni(COD)$_2$ (110 mg, 0.400 mmol, 2.00 equiv), and C_6H_6 (5 mL). The reaction mixture was stirred at ambient temperature for 24 h. A dark green color was observed within the first minute of the reaction. The solution then gradually turned dark brown over the 24 h period. The reaction mixture was then filtered through a glass fiber pad, and the filtrate was concentrated to dryness under reduced pressure. The residue was redissolved in C_6H_6 and concentrated two additional times to drive off any COD that remained bound to the complex. The solid residue was washed with three 1 mL portions of pentane. After drying under reduced pressure, ($^{i\text{-Pr}}$NDI)$Ni_2(C_6H_6)$ **2** (133 mg, 0.184 mmol, 92% yield) was isolated as a brown powder. Single crystals suitable for XRD were obtained by slow evaporation of a pentane solution. ^{1}H NMR (300 MHz, C_6D_6) δ 7.25−7.03 (m, 6H), 6.58 (d, J = 8.1 Hz, 2H), 5.91 (d, J = 8.1 Hz, 2H), 4.54 (s, 6H), 2.93 (sept, J = 6.8 Hz, 4H), 1.75 (s, 6H), 1.17 (d, J = 6.9 Hz, 12H), 0.93 (d, J = 6.8 Hz, 12H). ^{13}C NMR (75 MHz, C_6D_6) δ 176.2, 154.1, 144.9, 142.4, 139.0, 138.3, 126.1, 125.9, 123.9, 111.2, 79.4, 28.4, 25.4, 24.5, 16.4. UV−vis−NIR (THF, nm {M^{-1} cm^{-1}}): 240 {sh}, 302 {27 000}, 386 {21 000}, 416 {sh}, 506 {8900}, 1040 {40 000}. Anal. Calcd for **2** ($C_{42}H_{50}N_4Ni_2$): C 69.27, H 6.92, N 7.69; found: C 69.65, H 7.10, N 7.39%.

$(THF)_3K$($^{i\text{-Pr}}$NDI)$Ni_2(C_6H_6)$ (3). Under an atmosphere of N_2, a vial was charged with KC_8 (4.1 mg, 0.030 mmol, 1.0 equiv), ($^{i\text{-Pr}}$NDI)-$Ni_2(C_6H_6)$ **2** (21.7 mg, 0.0300 mmol, 1.00 equiv), and THF (2 mL). The reaction mixture was stirred at room temperature for 1 h, during which time a subtle color change from red-brown to yellow-brown was observe. The mixture was concentrated to dryness under reduced pressure. The residue was redissolved in a minimal amount of THF (approximately 1 mL) and filtered through a glass fiber pad. Diffusion of pentane vapor into the concentrated THF solution over a 24 h period yielded dark brown crystals. After decanting the mother liquor, washing the crystals with three 1 mL portions of pentane, and drying under vacuum, $(THF)_3K$($^{i\text{-Pr}}$NDI)$Ni_2(C_6H_6)$ **3** (12.2 mg, 0.0120 mmol, 42% yield) was isolated as a dark brown solid. Single crystals produced according to this procedure were suitable for XRD analysis. Complex **3** was observed to be NMR-silent. Simulated EPR parameters (298 K, THF): g_{iso} = 2.096; (125 K, THF): g_1 = 2.037, g_2 = 2.097, g_3 = 2.157. μ_{eff} = 1.4 μ_B (Evans method, 295 K, THF containing tetramethylsilane (TMS)). Anal. Calcd for **3** ($C_{54}H_{74}KN_4Ni_2O_3$): C 65.93, H 7.58, N 5.70; found: C 65.73, H 7.66, N 5.89%.

($^{i\text{-Pr}}$NDI)Ni_2Br_2 (4). Under an atmosphere of N_2, a Schlenk tube was charged with ($^{i\text{-Pr}}$NDI) **1** (107 mg, 0.200 mmol, 1.00 equiv), Ni(COD)$_2$ (55.0 mg, 0.200 mmol, 1.00 equiv), $NiBr_2$ (43.7 mg, 0.200 mmol, 1.00 equiv), and THF (5 mL). The reaction mixture was stirred at 60 °C for 24 h, during which time a green color developed and all of the initially insoluble $NiBr_2$ was consumed. The reaction mixture was concentrated to dryness. The residue was redissolved in a minimal amount of THF (approximately 2 mL) and filtered through a glass fiber filter. An equal volume of C_6H_6 was added, and pentane (approximately 15 mL) was layered on the solution. After mixing over a period of 12 h, the solution was decanted from the crystalline solid. The solid was washed with three 2 mL portions of pentane and dried under reduced pressure. ($^{i\text{-Pr}}$NDI)Ni_2Br_2 **4** (107 mg, 0.130 mmol, 66% yield) was isolated as a dark green solid. A second crop of crystals (21.2 mg, 0.0260 mmol, 13% yield) was recovered from the mother liquor according to the same procedure. Single crystals suitable for XRD were obtained by slow diffusion of pentane vapor into a concentrated bromobenzene solution. ^{1}H NMR (300 MHz, C_6D_6) δ 71.59, 32.85, 17.56, 14.71, 3.90, 3.10, −11.12, −75.85. UV−vis (THF, nm {M^{-1} cm^{-1}}): 265 {30 000}, 320 {sh}, 580 {sh}, 675 {5600}. μ_{eff} = 2.7 μ_B (Evans method, 295 K, THF containing TMS). Anal. Calcd for **4** ($C_{36}H_{44}Br_2N_4Ni_2$): C 53.38, H 5.48, N 6.92; found: C 53.67, H 5.31, N 6.80%.

($^{i\text{-Pr}}$NDI)Ni_2Br (5). Under an atmosphere of N_2, a vial was charged with ($^{i\text{-Pr}}$NDI)Ni_2Br_2 **4** (40.5 mg, 0.0500 mmol, 1.00 equiv), 0.5 wt % Na/Hg (1.3 mg, 0.055 mmol, 1.1 equiv dissolved in 250 mg of Hg),

dx.doi.org/10.1021/ic5020785 | Inorg. Chem. 2014, 53, 11770−11777

and THF (2 mL). After stirring for 1 h, the violet reaction mixture was filtered through a glass fiber pad to remove NaBr, and the filtrate was concentrated to dryness under reduced pressure. The residue was redissolved in a minimal amount of benzene and filtered a second time through a glass fiber pad (approximately 1 mL total volume of benzene). Pentane (10 mL) was layered on the concentrated benzene solution. After mixing for 12 h, the solution was decanted from the crystalline solid. The solid was washed with three 2 mL portions of pentane and dried under reduced pressure. After combining this material with a second crop of crystals obtained according to the same procedure, ($^{i\text{-Pr}}$NDI)Ni_2Br·1/2 C_6H_6 **5** (25.4 mg, 0.0350 mmol, 69% yield) was isolated as a dark violet solid. Single crystals suitable for XRD were obtained by diffusion of pentane vapor into a concentrated C_6H_6 solution. Complex **5** was observed to be largely NMR silent with the exception of broad singlets at 2.4 and 1.8 ppm. UV−vis (THF, nm {M^{-1} cm^{-1}}): 278 {39 000}, 360 {24 000}, 532 {13,000}, 601 {sh}, 796 {2400}. Simulated EPR parameters (298 K, 2-MeTHF): g_{iso} = 2.040; (125 K, 2-MeTHF): g_1 = 2.050, g_2 = 2.037, g_3 = 2.029. μ_{eff} = 1.6 μ_B (Evans method, 295 K, C_6H_6). Anal. Calcd for **5**·1/2 C_6H_6 ($C_{39}H_{47}BrN_4Ni_2$): C 60.90, H 6.16, N 7.28; found: C 61.20, H 5.97, N 7.34%.

[($^{i\text{-Pr}}$NDI)Ni_2(MeCN)$_2$$Br_2$]$PF_6$ (6). Under an atmosphere of N_2, a vial was charged with ($^{i\text{-Pr}}$NDI)Ni_2Br_2 **4** (24.3 mg, 0.0300 mmol, 1.00 equiv) and THF (2 mL). [Cp_2Fe][PF_6] (9.9 mg, 0.030 mmol, 1.0 equiv) in MeCN (2 mL) was added dropwise, causing the reaction solution to change from green to blue. After stirring for an additional 30 min, the mixture was concentrated to dryness. The residue was redissolved in MeCN and filtered through a glass fiber pad (approximately 1 mL total volume). Diffusion of Et_2O vapor into the concentrated MeCN solution over a period of 48 h yielded a dark blue crystalline solid. After decanting the mother liquor, washing the crystals with three 1 mL portions of Et_2O, and drying under vacuum, [($^{i\text{-Pr}}$NDI)Ni_2(MeCN)$_2$$Br_2$]$PF_6$ (22.6 mg, 0.0220 mmol, 73% yield) was isolated. Single crystals produced according to this procedure were suitable for XRD analysis. ^{1}H NMR (300 MHz, CD_3CN) δ 70.02, 69.68, 15.87, 10.59, 2.31, 1.45, −7.26, −49.54. UV−vis (THF, nm {M^{-1} cm^{-1}}): 254 {38 000}, 340 {15 000}, 680 {3100}. μ_{eff} = 4.1 μ_B (Evans method, 295 K, THF containing TMS). Anal. Calcd for **6** ($C_{40}H_{50}Br_2F_6N_4Ni_2P$): C 46.33, H 4.86, N 8.10; found: C 46.26, H 4.77, N 8.12%.

■ ASSOCIATED CONTENT

Ⓢ Supporting Information

Spectra, crystallographic details, and calculated structures. This material is available free of charge via the Internet at http://pubs.acs.org.

■ AUTHOR INFORMATION

Corresponding Author

*E-mail: cuyeda@purdue.edu.

Notes

The authors declare no competing financial interest.

■ ACKNOWLEDGMENTS

This work was generously supported by Purdue Univ. We thank S. Opperwall for experimental assistance with NIR measurements.

■ REFERENCES

(1) (a) Netherton, M. R.; Fu, G. C. *Adv. Synth. Catal.* **2004**, *346*, 1525−1532. (b) Montgomery, J. *Angew. Chem., Int. Ed.* **2004**, *43*, 3890−3908. (c) Rosen, B. M.; Quasdorf, K. W.; Wilson, D. A.; Zhang, N.; Resmerita, A.-M.; Garg, N. K.; Percec, V. *Chem. Rev.* **2010**, *111*, 1346−1416. (d) Hu, X. *Chem. Sci.* **2011**, *2*, 1867−1886.

(2) (a) Werner, H. In *Advances in Organometallic Chemistry;* Stone, F. G. A., Robert, W., Eds.; Academic Press: Waltham, MA, 1981; Vol. *19*, pp 155−182. (b) Murahashi, T.; Kurosawa, H. *Coord. Chem. Rev.* **2002**, *231*, 207−228. (c) Christmann, U.; Pantazis, D. A.; Benet-Buchholz, J.; McGrady, J. E.; Maseras, F.; Vilar, R. *J. Am. Chem. Soc.* **2006**, *128*, 6376−6390. (d) Hruszkewycz, D. P.; Wu, J.; Green, J. C.; Hazari, N.; Schmeier, T. J. *Organometallics* **2011**, *31*, 470−485. (e) Hruszkewycz, D. P.; Wu, J.; Hazari, N.; Incarvito, C. D. *J. Am. Chem. Soc.* **2011**, *133*, 3280−3283. (f) Hazari, N.; Hruszkewycz, D. P.; Wu, J. *Synlett* **2011**, *2011*, 1793−1797. (g) Powers, D. C.; Ritter, T. *Acc. Chem. Res.* **2011**, *45*, 840−850.

(3) (a) Powers, D. C.; Ritter, T. *Nat. Chem.* **2009**, *1*, 302−309. (b) Powers, D. C.; Geibel, M. A. L.; Klein, J. E. M. N.; Ritter, T. *J. Am. Chem. Soc.* **2009**, *131*, 17050−17051. (c) Deprez, N. R.; Sanford, M. S. *J. Am. Chem. Soc.* **2009**, *131*, 11234−11241.

(4) (a) Velian, A.; Lin, S.; Miller, A. J. M.; Day, M. W.; Agapie, T. *J. Am. Chem. Soc.* **2010**, *132*, 6296−6297. (b) Keen, A. L.; Johnson, S. A. *J. Am. Chem. Soc.* **2006**, *128*, 1806−1807. (c) Beck, R.; Johnson, S. A. *Chem. Commun.* **2011**, *47*, 9233−9235.

(5) (a) Pap, J. S.; DeBeer George, S.; Berry, J. F. *Angew. Chem., Int. Ed.* **2008**, *47*, 10102−10105. (b) Thomas, C. M.; Napoline, J. W.; Rowe, G. T.; Foxman, B. M. *Chem. Commun.* **2010**, *46*, 5790−5792. (c) Powers, T. M.; Fout, A. R.; Zheng, S.-L.; Betley, T. A. *J. Am. Chem. Soc.* **2011**, *133*, 3336−3338. (d) Mazzacano, T. J.; Mankad, N. P. *J. Am. Chem. Soc.* **2013**, *135*, 17258−17261. (e) Tereniak, S. J.; Carlson, R. K.; Clouston, L. J.; Young, V. G.; Bill, E.; Maurice, R.; Chen, Y.-S.; Kim, H. J.; Gagliardi, L.; Lu, C. C. *J. Am. Chem. Soc.* **2013**, *136*, 1842−1855.

(6) (a) Lin, S.; Agapie, T. *Synlett* **2011**, *2011*, 1−5. (b) Chao, S. T.; Lara, N. C.; Lin, S.; Day, M. W.; Agapie, T. *Angew. Chem., Int. Ed.* **2011**, *50*, 7529−7532. (c) Horak, K. T.; Velian, A.; Day, M. W.; Agapie, T. *Chem. Commun.* **2014**, *50*, 4427−4429. (d) Wu, J.; Nova, A.; Balcells, D.; Brudvig, G. W.; Dai, W.; Guard, L. M.; Hazari, N.; Lin, P. H.; Pokhrel, R.; Takase, M. K. *Chem.−Eur. J.* **2014**, *20*, 5327−5337. (e) DeLaet, D. L.; Del Rosario, R.; Fanwick, P. E.; Kubiak, C. P. *J. Am. Chem. Soc.* **1987**, *109*, 754−758. (f) Ferrence, G. M.; Simón-Manso, E.; Breedlove, B. K.; Meeuwenberg, L.; Kubiak, C. P. *Inorg. Chem.* **2004**, *43*, 1071−1081. (g) Beck, R.; Shoshani, M.; Krasinkiewicz, J.; Hatnean, J. A.; Johnson, S. A. *Dalton Trans.* **2013**, *42*, 1461−1475. (h) Beck, R.; Johnson, S. A. *Organometallics* **2013**, *32*, 2944−2951.

(7) (a) Bart, S. C.; Chłopek, K.; Bill, E.; Bouwkamp, M. W.; Lobkovsky, E.; Neese, F.; Wieghardt, K.; Chirik, P. J. *J. Am. Chem. Soc.* **2006**, *128*, 13901−13912. (b) Muresan, N.; Chlopek, K.; Weyhermüller, T.; Neese, F.; Wieghardt, K. *Inorg. Chem.* **2007**, *46*, 5327−5337. (c) Lu, C. C.; Bill, E.; Weyhermüller, T.; Bothe, E.; Wieghardt, K. *J. Am. Chem. Soc.* **2008**, *130*, 3181−3197.

(8) (a) Darmon, J. M.; Stieber, S. C. E.; Sylvester, K. T.; Fernández, I.; Lobkovsky, E.; Semproni, S. P.; Bill, E.; Wieghardt, K.; DeBeer, S.; Chirik, P. J. *J. Am. Chem. Soc.* **2012**, *134*, 17125−17137. (b) Bouwkamp, M. W.; Bowman, A. C.; Lobkovsky, E.; Chirik, P. J. *J. Am. Chem. Soc.* **2006**, *128*, 13340−13341. (c) Jones, G. D.; Martin, J. L.; McFarland, C.; Allen, O. R.; Hall, R. E.; Haley, A. D.; Brandon, R. J.; Konovalova, T.; Desrochers, P. J.; Pulay, P.; Vicic, D. A. *J. Am. Chem. Soc.* **2006**, *128*, 13175−13183.

(9) (a) Zhou, J.; Fu, G. C. *J. Am. Chem. Soc.* **2003**, *125*, 14726−14727. (b) Everson, D. A.; Shrestha, R.; Weix, D. J. *J. Am. Chem. Soc.* **2010**, *132*, 920−921. (c) Everson, D. A.; Jones, B. A.; Weix, D. J. *J. Am. Chem. Soc.* **2012**, *134*, 6146−6159.

(10) (a) Fischer, C.; Fu, G. C. *J. Am. Chem. Soc.* **2005**, *127*, 4594−4595. (b) Arp, F. O.; Fu, G. C. *J. Am. Chem. Soc.* **2005**, *127*, 10482−10483. (c) Son, S.; Fu, G. C. *J. Am. Chem. Soc.* **2008**, *130*, 2756−2757. (d) Smith, S. W.; Fu, G. C. *J. Am. Chem. Soc.* **2008**, *130*, 12645−12647.

(11) (a) Bera, J. K.; Sadhukhan, N.; Majumdar, M. *Eur. J. Inorg. Chem.* **2009**, *2009*, 4023−4038. (b) Tikkanen, W. R.; Binamira-Soriaga, E.; Kaska, W. C.; Ford, P. C. *Inorg. Chem.* **1983**, *22*, 1147−1148. (c) He, C.; Lippard, S. J. *Inorg. Chem.* **2000**, *39*, 5225−5231. (d) Campos-Fernández, C. S.; Ouyang, X.; Dunbar, K. R. *Inorg. Chem.* **2000**, *39*, 2432−2433. (e) Campos-Fernández, C. S.; Thomson, L. M.; Galán-Mascarós, J. R.; Ouyang, X.; Dunbar, K. R. *Inorg. Chem.* **2002**, *41*, 1523−1533. (f) Davenport, T. C.; Tilley, T. D. *Angew. Chem., Int. Ed.* **2011**, *50*, 12205−12208.

(12) (a) Lan, Y.; Kennepohl, D. K.; Moubaraki, B.; Murray, K. S.; Cashion, J. D.; Jameson, G. B.; Brooker, S. *Chem.—Eur. J.* **2003**, *9*, 3772−3784. (b) Roder, J. C.; Meyer, F.; Pritzkow, H. *Chem. Commun.* **2001**, 2176−2177. (c) Ziessel, R.; Harriman, A.; El-ghayoury, A.; Douce, L.; Leize, E.; Nierengarten, H.; Van Dorsselaer, A. *New J. Chem.* **2000**, *24*, 729−732.
(13) Dible, B. R.; Sigman, M. S.; Arif, A. M. *Inorg. Chem.* **2005**, *44*, 3774−3776.
(14) For selected examples of multinuclear complexes without metal-metal bonds exhibiting multiple reversible redox events: (a) Szymczak, N. K.; Berben, L. A.; Peters, J. C. *Chem. Commun.* **2009**, 6729−6731. (b) Blusch, L. K.; Craigo, K. E.; Martin-Diaconescu, V.; McQuarters, A. B.; Bill, E.; Dechert, S.; DeBeer, S.; Lehnert, N.; Meyer, F. *J. Am. Chem. Soc.* **2013**, *135*, 13892−13899. (c) Feke Maloney, S. C.; McDevitt, M. R.; Urbach, F. L. *Inorg. Chim. Acta* **1989**, *164*, 123−125. (d) Brooker, S.; Davidson, T. C.; Hay, S. J.; Kelly, R. J.; Kennepohl, D. K.; Plieger, P. G.; Moubaraki, B.; Murray, K. S.; Bill, E.; Bothe, E. *Coord. Chem. Rev.* **2001**, *216−217*, 3−30.
(15) (a) Geßner, C.; Stein, M.; Albracht, S. P. J.; Lubitz, W. *J. Biol. Inorg. Chem.* **1999**, *4*, 379−389. (b) Trofanchuk, O.; Stein, M.; Geßner, C.; Lendzian, F.; Higuchi, Y.; Lubitz, W. *J. Biol. Inorg. Chem.* **2000**, *5*, 36−44. (c) Marr, A. C.; Spencer, D. J. E.; Schröder, M. *Coord. Chem. Rev.* **2001**, *219−221*, 1055−1074.
(16) (a) Newkome, G. R.; Garbis, S. J.; Majestic, V. K.; Fronczek, F. R.; Chiari, G. *J. Org. Chem.* **1981**, *46*, 833−839. (b) Zong, R.; Wang, D.; Hammitt, R.; Thummel, R. P. *J. Org. Chem.* **2005**, *71*, 167−175.
(17) Stoll, S.; Schweiger, A. *J. Magn. Reson.* **2006**, *178*, 42−55.
(18) Spek, A. L. *Acta Crystallogr., Sect. D* **2009**, *65*, 148−155.
(19) Frisch, M. J.et al. *Gaussian 09,* Revision D.01; Gaussian, Inc.: Wallingford, CT, 2009.
(20) (a) Becke, A. D. *J. Chem. Phys.* **1986**, *84*, 4524−4529. (b) Perdew, J. P.; Yue, W. *Phys. Rev. B* **1986**, *33*, 8800−8802. (c) Perdew, J. P. *Phys. Rev. B* **1986**, *33*, 8822−8824. (d) Ditchfield, R.; Hehre, W. J.; Pople, J. A. *J. Chem. Phys.* **1971**, *54*, 724−728. (e) Hehre, W. J.; Ditchfield, R.; Pople, J. A. *J. Chem. Phys.* **1972**, *56*, 2257−2261. (f) Hariharan, P. C.; Pople, J. A. *Theoret. Chim. Acta* **1973**, *28*, 213−222.